Feasibility Study of a New Model for the Thermal Boundary Resistance at an Interface of Solid Thin Films

Soon Ho Choi* and Shigeo Maruyama**
Department of Mechanical Engineering, The University of Tokyo, Tokyo, Japan

The thermal boundary resistance (TBR) is still a challengeable subject since its mechanism to explain quantitatively is not clear in spite of its importance. We performed non-equilibrium molecular dynamic (NEMD) simulation to evaluate TBR at an epitaxial solid interface composed of two different materials. Solid argon is selected as a simulation material since it is a non-conductor electrically, so that energy transportation is caused only by lattice vibration. The history to grasp the mechanism on TBR is fairly long and the various theories were developed such as an acoustic mismatch model (AMM), an acoustic impedance mismatch model (AIMM) and a diffuse mismatch model (DMM), however any model can't make a success of analyzing TBR quantitatively. The mechanism of TBR can be explained as the energy reflection at an interface caused by the discontinuity of acoustic impedance even in a microscale system from this study. However it should be corrected with the consideration of a microscale characteristic. The corrected microscale acoustic impedance mismatch model (CM-AIMM), which is developed in this study, fairly well predicts TBR compared with any other existing models.

I. INTRODUCTION
*

The nano- and micro-technologies have been more critical to the related industries such as a semi-conductor, a micro-electromechanical system (MEMS) and a nano-electromechanical system (NEMS). These newly growing technologies make the various devices perform the advanced functions with a more reduced size and change even the human life [1]. However these new technologies require at the same time that we should thoroughly understand, analyze the new phenomena resulted from the extremely small size and the application limits of the existing theories based on a macro system [2-13].

In MEMS and NEMS the thermal boundary resistance (TBR) at a solid interface composed of two different materials or a grain boundary is focused one's attention [3-14] because it plays key role in the heat dissipation capacity of those devices. For example the heat generation from CPU or an electronic chip degrades the performance of them, so that a proper heat removal is very important to assure their designed functions. However the existence of an interface between a substrate and a mounted chip on it prevents from flowing out a heat current, which causes a device to fail an intended performance or a proper operation.

Recent thin film deposition technology, which is able to control to the range of one atom thickness nowadays, makes supperlattices be possible as shown in Fig. 1. This material is an artificial film not existed in nature since it is possible to be manufactured from arbitrary selections of any element [15]. Many studies report that there are two manifest features in a thermal phenomenological sense. One is that there is a large temperature jump at an interface in supperlattices and the other is that the thermal conductivity of each film is lower than that in a bulk state [16-21]. The latter is relatively well explained and analyzed by the concept of a phonon mean free path (MFP) in Ref. 2 submitted with this paper [2]. However it can be said within our knowledge at least that there is no theory to explain quantitatively the magnitude of TBR at a solid interface, so that it remains still a challengeable subject [3-21] since Kapitza found the existence of TBR at an interface between the metal surface and liquid Helium [1-2].

After Kapitza's observation of TBR, many researchers have focused all their attention on TBR between solid-liquid or solid-solid interface. The first attempt to explain the mechanism of TBR was done by Little [5] who applied the concept of a phonon reflection and transmission at a solid-solid interface, which is now called as an acoustic mismatch model (AMM). Hereafter the almost experimental or computational results were compared with the predictions based on AMM, however the comparisons were far from the quantitative agreement except in the case that the temperature of a system is lower than about 0.01 K [3-4, 6]. To overcome this discrepancy Swartz proposed a diffuse mismatch model that is called as DMM [3]. Although it shows a little improved prediction of a thermal conductance in the region of a high temperature, there is still a large gap between an experimental result and a prediction by DMM.

In contrast to a microscale situation, TBR seems to be considerably reduced from the results of a

* E-mail : choi@photon.t.u-tokyo.ac.jp
** E-mail: aruyama@photon.t.u-tokyo.ac.jp

macroscale system if the actual contacting area at an interface is increased by any method [22-26]. Those results make one understand that TBR is disappeared if the interface is perfect contact as shown in Fig. 1, which is considered as fairly reasonable. However, against our naive expectation, the recent study by Matumoto et al. reported that TBR still exists at an epitaxial interface between dissimilar materials even though an interface is perfectly contacted in view of an atomic level [27]. Matumoto's study was performed with changing the molecular mass of two species and a potential well depth ε, but failed to predict TBR quantitatively.

This study is carried out to develop a new model to predict TBR accurately using NEMD and investigated only the effect caused by a molecular mass ratio. Solid argon is selected as a simulation material because of the same reason described in another paper submitted with this [2]. It has been found from this study that TBR at an interface is explicitly dependent on the mass ratio between two different materials and the higher a mass ratio is the higher TBR. The mechanism of TBR can be explained as the energy reflection at an interface caused by the discontinuity of acoustic impedance. AIMM is corrected for the microscale system and it is confirmed to evaluate TBR qualitatively and quantitatively compared with any other model such as AMM, AIMM and DMM. The detailed description will be given in the next sections.

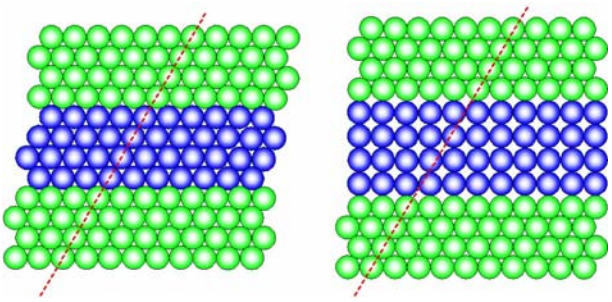

(a) Epitaxial Supperlattice (b) Non-epitaxial Supperlattice

Fig. 1. Schematic Cross Sections of Superlattices

II. SIMULATION METHOD

A simulation system is arranged with fcc <111> as shown in Fig. 2 and the simulation method is actually the same as described in Ref. 2 except that the upper half of a system has the different molecular mass from the lower half. The adiabatic wall of 3 layers and the temperature control layers (TCLs) are placed at both ends of a system. The former are for isolating the system from circumstances and the latter for controlling both TCLs to each desired temperature. The bottom is controlled to a high temperature and the top to a low temperature, so that a heat current flows up (z direction). The x-y plane perpendicular to the heat flow direction is set as a periodic boundary condition (PBC), which behaviors just as an actual thin film. The velocity scaling method is used for the temperature control of both TCLs and the equation of motion is integrated by the Velocity Verlet method in the same as Ref. 2. An intermolecular distance is determined to maintain a system to be under a freestanding state, which means a system to be in the zero stress state internally during a simulation [28-32]. The selected intermolecular length in this study is the same as Ref. 2.

Eighteen argon molecules are arranged on x and y direction respectively in one layer and total layer of a system is thirty in z direction. A temperature gradient is measured in the medium of the eighteen layers excluding the temperature control layers and the adiabatic wall at each side. Time interval for an iteration calculation is selected as $\Delta t=1.0\text{x}10^{-15}$ s (=1 fs) and the cut-off length an intermolecular interaction 3.5 σ_{AR}. The properties of argon are $\sigma_{AR}=3.4$ Å, $m_{AR}=6.634\text{x}10^{-26}$ kg and $\varepsilon_{AR}=1.67\text{x}10^{-21}$ J.

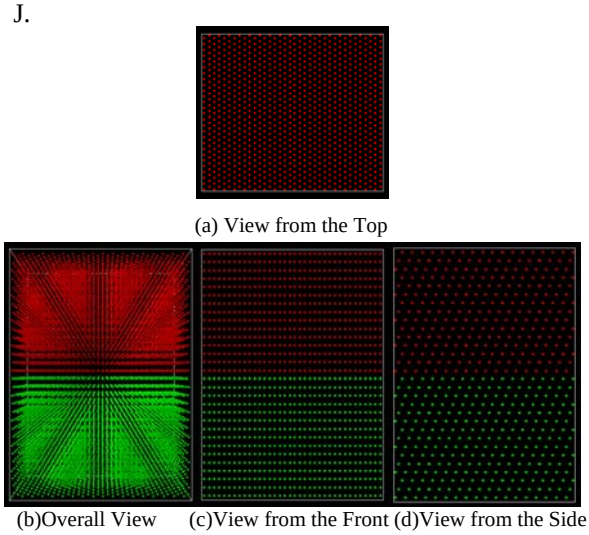

(a) View from the Top

(b)Overall View (c)View from the Front (d)View from the Side

(18 x 18 molecules in a plane and 30 layers in length)

Fig. 2. The Simulation System of fcc<111> with an Adiabatic Wall

The lower half of Fig. 2 is composed of the argon molecules to have the earlier specified properties, however the upper half the imaginary argon molecules that have a different mass. The latter has the same properties except for the mass, which make one evaluate TBR especially caused by the mass difference. TBR is investigated in case that the mass ratio is 1:2, 1:3, 1:5 and 1:7 respectively. The first simulation makes a system maintain an initial equilibrium state at any setting temperature and then controlling both TCLs respectively develops a temperature gradient in a system. These simulations are performed six times each of which is 400,000 iterations (400 ps), however the first one is excluded in the evaluation of a thermal conductivity since it must be a transient period to develop a temperature gradient in a system. Therefore the thermal conductivity is the averaged value over the rest five

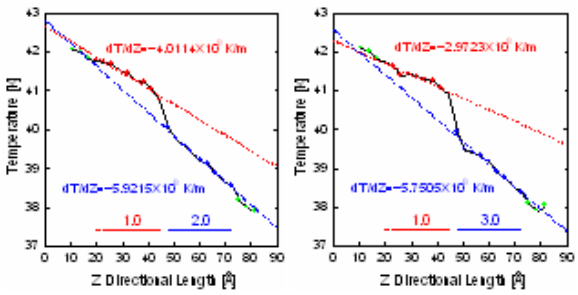

(a) Mass Ratio of 1:2 (T_{ave} ; 40.3 K)
(b) Mass Ratio of 1:3 (T_{ave} ; 40.2 K)
(c) Mass Ratio of 1:5 (T_{ave} ; 40.3 K)
(d) Mass Ratio of 1:7 (T_{ave} ; 40.2 K)

Fig. 3. Temperature Jump at Interface by Different Mass Ratio

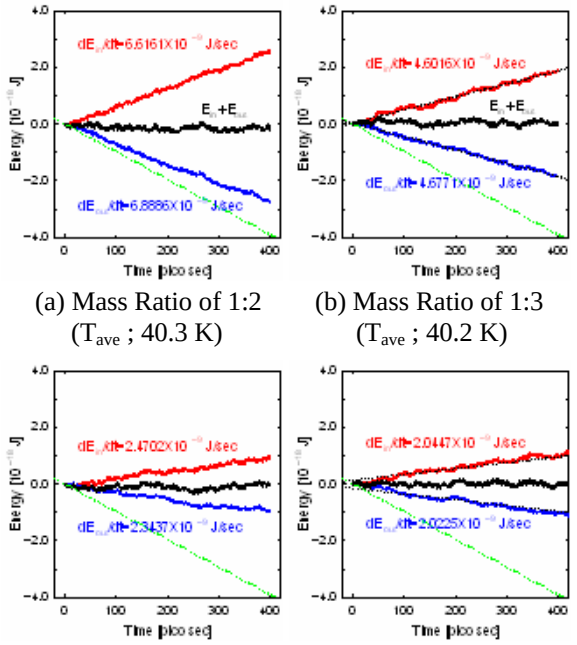

(a) Mass Ratio of 1:2 (T_{ave} ; 40.3 K)
(b) Mass Ratio of 1:3 (T_{ave} ; 40.2 K)
(c) Mass Ratio of 1:5 (T_{ave} ; 40.3 K)
(d) Mass Ratio of 1:7 (T_{ave} ; 40.2 K)

Fig. 4. Heat Flux Reductions by Different Mass Ratio

simulations. The initial equilibrium temperature is 40 K. During all simulations for developing a temperature gradient the high TCLs is controlled to 42 K and the low TCLs to 38 K always (ΔT=4 K). It is confirmed that the averaged temperature of a system is maintained to 40 K during all simulations although each TCLs is in the different setting temperature, that is 38 K and 40 K.

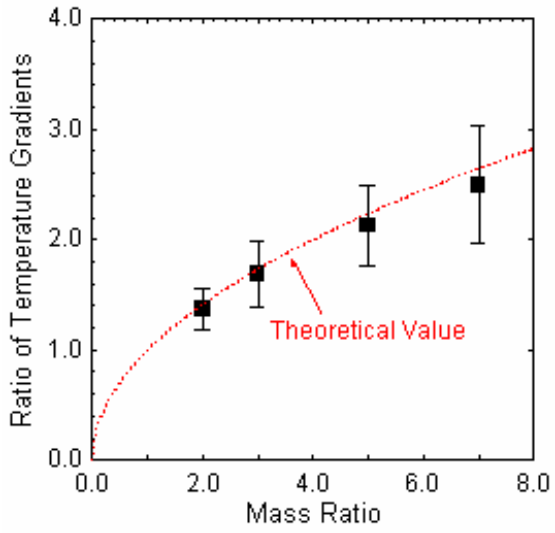

Fig. 5. Temperature Gradient Ratio of the System with a Mass Ratio

III. RESULTS AND DISCUSSION

III-I. TEMPERATURE JUMP AT AN INTERFACE AND HEAT FLUX

There is no need to describe the method of the calculation of a heat flux, a thermal conductivity and the determination of an intermolecular length here repeatedly since the details of them are explained in Ref. 2. From the simulation results it is observed that a heat flux is reduced and a temperature jump is increased when a mass ratio gets more increased as our expectation. Fig. 3 and Fig. 4 shows respectively the examples of the temperature jump at an interface and the heat flux of each corresponding mass ratio. It is clear that the heat current is prevented from flowing through an interface owe to the increased TBR as the mass ratio is increased. The thick dotted line on Fig. 4 is the heat flux of a system in which all molecules are argon, that is no interface. Heat inflow and outflow by the velocity scaling of both TCLs are almost the same (maximum 3 % deviation), which justifies that the system is fully under a non-equilibrium steady state during a simulation.

The theoretical ratio of two temperature gradients of a system as shown in Fig. 3 can be calculated from the definition of a dimensionless thermal conductivity [29-30].

$$\lambda^* = -\dot{q}\frac{\Delta L}{\Delta T}\left\{\frac{\sigma^2}{k_B}\sqrt{\frac{m}{\varepsilon}}\right\} = \lambda\left\{\frac{\sigma^2}{k_B}\sqrt{\frac{m}{\varepsilon}}\right\} \qquad (1)$$

In Eq. (1) $\dot{q}$ is a heat flux, ΔL a system length, ΔT the temperature difference between both ends and k_B is the Boltzmann constant, $1.38\text{x}10^{-23}$ J/K. Considering that the upper half and the lower half of a system have the same properties except for their mass, it is easily derived from Eq. (1) that the

theoretical ratio of two temperature gradients is proportional to the square root of a mass ratio.

$$\frac{\frac{\Delta T_2}{\Delta L}}{\frac{\Delta T_1}{\Delta L}} = \frac{\Delta T_2}{\Delta T_1} = \sqrt{\frac{m_2}{m_1}} \tag{2}$$

Fig. 5 is the measured ratios of the temperature gradients from all simulation and each data point are averaged over five simulations. It shows that the MD results are fairly well agreed with the theoretical value of Eq. (2) and the standard deviation ($1\cdot\sigma_{STD}$) is about 20 % of the average at most.

III-II. PREDICTION OF THERMAL BOUNDARY RESISTANCE BY AIMM

The history to grasp the mechanism of TBR is fairly long as described previously and the typical models are AMM and DMM, which are concerned with phonon transportation phenomena [3-5]. However it is well known that neither of them agrees with experimental data except for an extremely low temperature region although both models give rather similar predictions for many cases [6]. Moreover these models were too complicate to handle easily for engineering use. We don't mention the details of AMM and DMM again since other references provide with the full description on these models [3-4]. Recently Matumoto et al. tried to evaluate TBR by comparing with the heat fluxes between the reference system that consists of all the same molecules of argon (hereafter called as SYS_{REF1}) and the system that has a mass ratio (hereafter called as SYS_{MR}) [27]. The concept by Matymoto is very simple. They defined the energy reflection coefficient (ERC) from the above heat fluxes and then compared with ERC from an acoustic impedance mismatch model (AIMM). As well known, AIMM is the model for calculating ERC occurred at an interface of a macroscale system considered as a continuum. If we assume that an incident wave to an interface is $A_1\cdot\exp\{i(\omega\cdot t-k_1\cdot x)\}$, a reflection wave from it $B_1\cdot\exp\{i(\omega\cdot t+k_1\cdot x)\}$ and a transmitted wave through it $A_2\cdot\exp\{i(\omega\cdot t-k_2\cdot x)\}$, then ERC is given as follows [29-30, 33].

$$ERC = \left(\frac{1-\frac{\rho_2 c_2}{\rho_1 c_1}}{1+\frac{\rho_2 c_2}{\rho_1 c_1}}\right)^2 = \left(\frac{1-\frac{m_2 c_2}{m_1 c_1}}{1+\frac{m_2 c_2}{m_1 c_1}}\right)^2 \tag{3}$$

$$ERC = 1-\frac{\dot{q}_{MR}}{\dot{q}_{REF}} \tag{4}$$

In Eq. (4) $\dot{q}_{REF}$ is the heat flux of SYS_{REF1} and $\dot{q}_{MR}$ the heat flux of SYS_{MR}. The acoustic velocity of a solid material, *c* is theoretically the square root of a ratio of Young's modulus to a density. Since Young's modulus is related with a potential well, ε and two species are assumed to have the same potential well in this study, Eq.(4) can be rewritten as Eq. (5).

$$ERC = \left(\frac{1-\sqrt{\frac{m_2}{m_1}}}{1+\sqrt{\frac{m_2}{m_1}}}\right)^2 \tag{5}$$

Matumoto et al. supposed that ERC by the heat flux ratio of Eq. (4) is equal to ERC by AIMM of Eq. (5), however their MD results were largely different from the prediction by Eq. (5). Although the attempt by them showed not to predict TBR quantitatively it is worthwhile noting their concept because it is very simple and shows a little improved estimation of TBR compared with AMM or DMM. We investigated their concept thoroughly from the starting point of AIMM theory and found that it can be an excellent model to anticipate TBR if it is corrected for a microscale system. This will be described in the next section.

III-III. CORRECTED MICROSCALE ACOUSTIC IMPEDANCE MISMATCH MODEL (CM-AIMM)

As mentioned previously the method of Matumoto's et al. is very simple to understand and easy to handle while it fails to predict TBR quantitatively. It may be considered that the discrepancy between MD results and AIMM prediction results from the direct application of AIMM to a microscale system without any consideration. If we consider the fact that AIMM was originally developed for a macro system, it is reasonable that some assumptions should be corrected for applying AIMM to a microscale system. AIMM was developed under two boundary conditions (BCs) of (1) the displacements of both sides at an interface are the same immediately for all time and (2) the force acting to both sides at an interface are also the same. These conditions assure that there is no discontinuity of the displacement and the force at an interface. However it is questionable that BC (1) is applicable to a microscale system though BC (2) is considered to be reasonable still.

Under our assumptions the displacements of molecules are not collective but rather random from a microscopic viewpoint. In a macroscale system such as a string, a slender bar or a slinky the imparted energy for a wave motion is extremely large compared with the energy of a molecular motion, so that the energy by the molecular motions can be ignored completely. Therefore ERC can be calculated sufficiently considering only the collective motion of a body. However in a microscale system like this study the energy transport depends only on the thermal motions from the molecules and it must be

considered when evaluating TBR. Supposing two molecules with a different mass respectively under the Lennard-Jones (L-J) potential and their movements, it can be easily imagined that the amplitudes of two molecules are different from each other and expected to be proportional to each mass.

Fig. 6 shows the respective amplitudes of each with the different mass, which are measured from each equilibrium position during a motion. It is concluded from this figure that our assumption can be accepted for a correction of AIMM. Consequently BC (1) should be corrected for a microscale system as (1) the displacements of both sides at an interface has the ratio proportional to their mass ratio for all time. Under these corrected BCs, ERC by AIMM is derived as Eq. (6).

$$ERC = \left(\frac{1-\alpha \cdot \frac{Z_2}{Z_1}}{1+\alpha \cdot \frac{Z_2}{Z_1}} \right)^2 \quad \begin{bmatrix} \alpha = m_2 / m_1 \\ Z = \rho c \end{bmatrix} \tag{6}$$

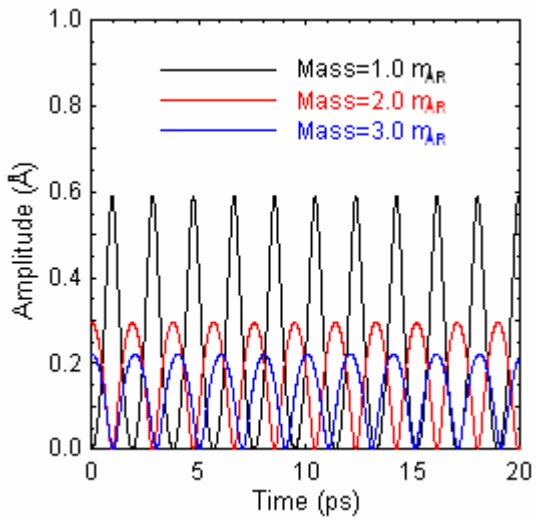

Fig. 6. Amplitude of Two molecules with Different Mass under the L-J potential

In Eq. (6) Z is acoustic impedance that is the product of the density and the acoustic velocity of a material. Eq. (6) is named as CM-AIMM in this study and it is identical with Eq. (3) if α is replaced as 1.0. Before applying Eq.(6) to a microscale system, it should be considered what system can be regarded as a reference. Matumoto et al. considered that a reference system is SYS_{REF1} under the same simulation conditions. However the system with a mass ratio is certainly different from one without a mass ratio even though the same simulation conditions are applied such as the same physical dimensions and the temperature difference at both ends. Rather the reference of a simulation system may well be own itself to be assumed without the temperature jump at an interface (hereafter called as SYS_{REF2}), which is easily created from Eq.(2).

Figure 7 (a) is the example of MD simulation in case that the mass ratio is 1:2 and (b) the simplified temperature profile of (a). If there is no temperature jump at an interface of a simulation system, T_A must be decreased and T_B increased as shown in (b). However the corrected temperature gradient should satisfy the following relationships.

$$\Delta T_{GAP} = \Delta T_A + \Delta T_B \tag{7}$$

$$\Delta T_A = \frac{\Delta T_{GAP}}{\left(1+\sqrt{\frac{m_2}{m_1}}\right)} \tag{8}$$

$$\Delta T_B = \frac{\Delta T_{GAP}\sqrt{\frac{m_2}{m_1}}}{\left(1+\sqrt{\frac{m_2}{m_1}}\right)} \tag{9}$$

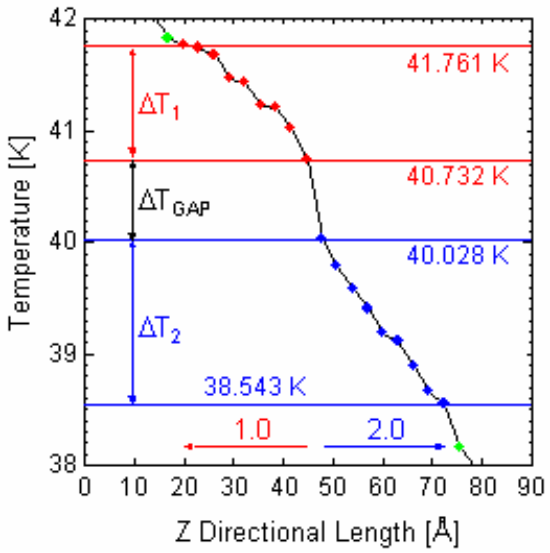

(a) Measured Temperature Profile by MD

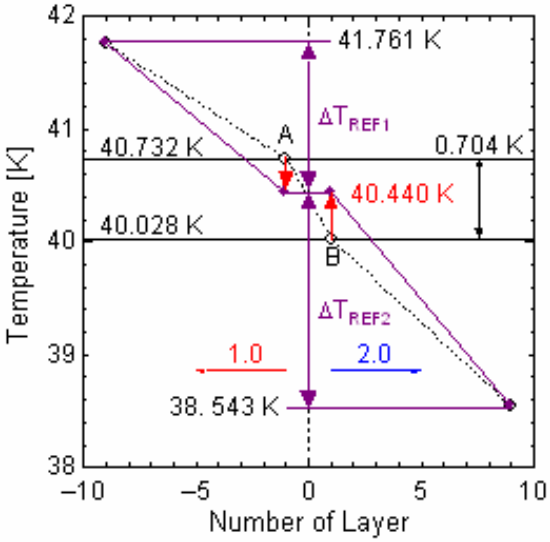

(b) Simplified Temperature Profile

Fig. 7. Temperature Profile of the Reference System

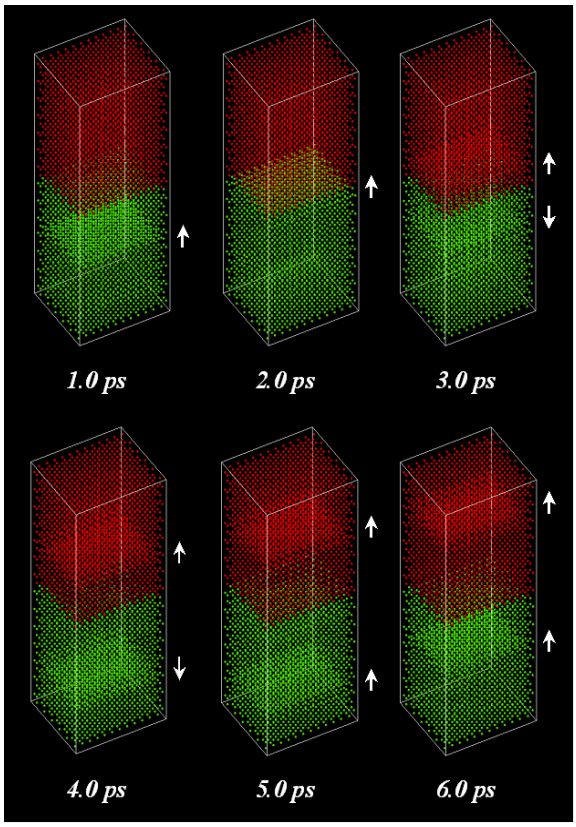

Fig. 8. Wave Behavior in the System with an Interface

Assuming that there is no temperature jump at an interface, the heat flux of SYS_{REF2} must be increased compared with SYS_{MR} and it can be calculated from the ratio of the corrected temperature difference to the originally measured one by MD simulation.

$$\frac{\dot{q}_{REF2}}{\dot{q}_{MR}} = \frac{\Delta T_{REF1}}{\Delta T_1} = \frac{\Delta T_{REF2}}{\Delta T_2} \tag{10}$$

In Eq. (10) $\dot{q}_{REF}$ is the heat flux of SYS_{REF2} and $\dot{q}_{MR}$ the heat flux of SYS_{MR}. As a result, ERC by the concept of a reference system is calculated by subtracting the reverse of Eq. (10) from unit.

$$ERC = 1 - \frac{\Delta T_1}{\Delta T_{REF1}} = 1 - \frac{\Delta T_2}{\Delta T_{REF2}} \tag{11}$$

In this study Eq. (11), which is a result by MD simulation and corresponds to an actual experiment, is compared with the theoretical ERC by CM-AIMM of Eq. (6). However it is necessary that the acoustic impedance of a material should be determined before calculating ERC. For this purpose we prepared the long system of fcc <111> arrangement and imparted a weak pulse to the bottom after achieving an initial equilibrium state. From the observation of the kinetic energy of a system we measured the acoustic velocity. Fig. 8 is the snapshots that show the reflection and transmission of a wave occurred at an interface. The z directional displacements of the molecules were exaggerated for the visualization. Fig. 9 is the kinetic energy behaviors of each layer with the time and corresponds to Fig. 8.

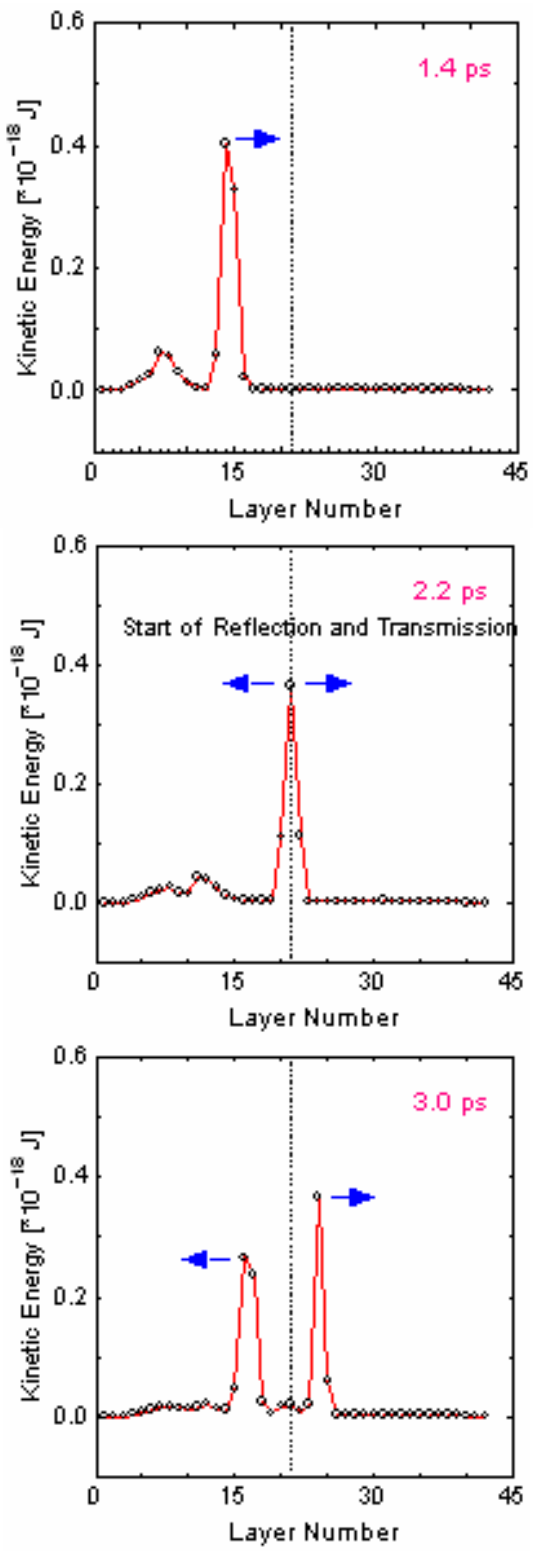

Fig. 9. Kinetic Energy Behavior of a Layer in the System with an Interface

From the previous results of Fig. 8 and 9 we calculated the acoustic velocity of each material and

confirmed that the mechanism of TBR is reasonable, which is caused by a wave reflection at an interface. The measured acoustic velocity is different from the theoretical prediction that is proportional to the square root of the ratio of Young's modulus to a density. Fig. 10 is the observed value of the acoustic velocity with the change of a mass and resulted in the power of 0.6 approximately.

Fig. 11 shows ERC results of this study, in which the dotted line is ERC by AIMM calculated from Eq. (3) and the solid line is that by the CM-AIMM from Eq. (6). Both theoretical values are based on the measured acoustic velocity of Fig. 10 and tabulated in Table 1. The opened circle is the ERC by Matumoto et al., which was on the system arranged with fcc<100> and the heat flux ratio between SYS_{MR}

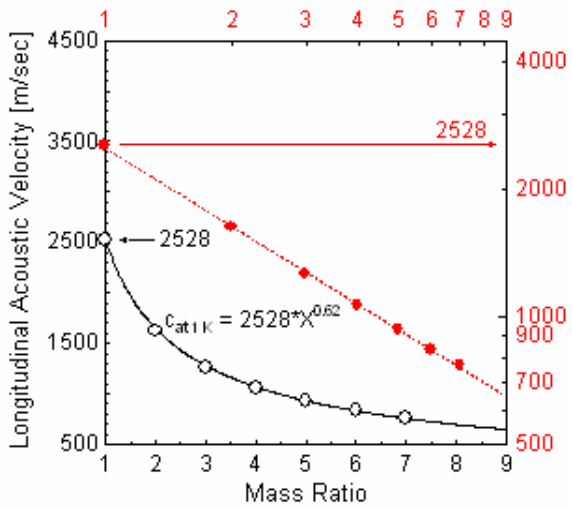

Fig. 10. Measurement of Acoustic Velocity

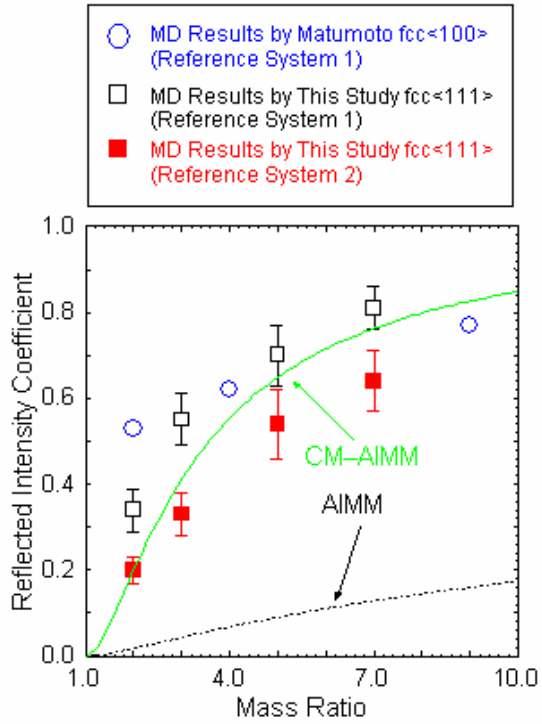

Fig. 11. Comparison of ERC by Each Model

TABLE 1: Comparison of ERC among the Theoretical Values and MD Results

Mass Ratio	ERC from Matumoto et al.	ERC from this Study	ERC by AIMM	ERC by CM-AIMM
1:2	53 %	20 %	5 %	20 %
1:3	---	33 %	7 %	41 %
1:4	62 %	---	11 %	55 %
1:5	---	54 %	15 %	65 %
1:7	---	64 %	20 %	76 %
1:9	77 %	---	25 %	83 %

and SYS_{REF1}. The opened square is the ERC by this study and also based on the heat flux ratio as same as the above. The solid square is ERC by this study however they are based on the heat flux ratio between SYS_{MR} and SYS_{REF2}, which is assumed that there is no temperature jump at an interface. As seen in Figure 11, it is clear that the developed CM-AIMM, which is based on the concept of the reflection of an incident wave or energy at an interface, predicts well TBR compared with any other model. Moreover this new model can evaluate the temperature profile through Eq.(7) to (9). Considering the results of this study, it is supposed that AIMM based on a macroscal system is still applicable to a microscale system if a proper coefficient is introduced. Indeed a correction coefficient α of Eq. (6) plays such a role. Therefore it can be explained that the reported discrepancy between the experiments and the theoretical models such as AMM, DMM and AIMM results from ignoring the characteristic of a molecular motion when measuring TBR at an interface between thin solid film.

IV. CONCLUSION

The molecular dynamics simulation is performed to analyze the TBR at an interface of a system with different materials and it is confirmed that the mechanism of TBR can be explained by the concept of a classical wave theory in which an incident wave is partly reflected and partly transmitted on an interface. Some correction is made to a conventional AIMM for a macro system and the new concept, which is the heat flux ratio between a simulation system and a reference system, is introduced to evaluate TBR. The CM-AIMM developed in this study predicts TBR accurately compared with other existing models such as AMM, DMM and AIMM. The maximum deviation between the ERCs by CM-AIMM and MD results within 12 %, which is the case of the mass ratio of 1:7. This is quite satisfactory result for engineering use. Moreover this new model

can evaluate the temperature jump occurred at an interface through Eq.(7) to (9). However it must be noted that this study is insufficient since this does not contain any effect resulted from an intermolecular potential. Further study will be performed for including it to the CM-AIMM.

REFERENCES

[1] S.E. Lyshevski, Nano- and Microelectro mechanical Systems (CRC press, New York, 2001).

[2] S.H. Choi et al., submitted to J. Kor. Phys. Soc. with this paper (2003).

[3] E.T. Swartz and R. O. Pohl, Rev. Mod. Phys., **61**, 605 (1989).

[4] David G. Cahill et al., J. Appl. Phy., **93**, 793 (2003).

[5] W.A. Little, Canadian J. Phys., **37**, 334 (1959).

[6] P.E. Phelan, ASME J. Heat Transfer, **120**, 37 (1998).

[7] E.T. Swartz and R. O. Pohl, Appl. Phys. Lett., **51**, 2200 (1987).

[8] M. Asheghi et al, Appl. Phys. Lett., **71**, 1798 (1997).

[9] Y.S. Ju and K.E. Goodson, Appl. Phys. Lett., **74**, 3005 (1999).

[10] R.J. Stoner and H.J. Maris, Phys. Rew. B, **48**, 16373 (1993).

[11] G. Chen, J. Nanoparticle Research, **2**, 199 (2000).

[12] G. Chen, ASME J. Heat Transfer, **119**, 220 (1997).

[13] A.R. Abramson, ASME J. Heat Transfer, **124**, 963 (2002).

[14] H.S. Yang et al., ACTA Materialia, **50**, 2309 (2002).

[15] Teruya Shinjo and Toshio Takada, Metallic Superlattices-Artificially Structured Materials (Elsevier, Amsterdam, 1987).

[16] Brian C. Daly and Humphrey J. Maris, Physica B, **316-317**, 247 (2002).

[17] G. Chen and M. Neagu, Appl. Phys. Lett., **71**, 2761 (1997).

[18] W.S. Capinski et al., Physica B, **263-264**, 530 (1999).

[19] Per Hyldgaard and G.D. Mahan, Phys. Rew. B, **56**, 10754 (1997).

[20] Takafumi Yao, Appl. Phys. Lett., **51**, 1798 (1987).

[21] X.Y. Yu and G. Chen, Appl. Phys. Lett., **67**, 3554 (1995).

[22] G.F.C. Roggers, Int. J. Heat & Mass Transfer, **2**, 150 (1961).

[23] R.W. Powell et al., Int. J. Heat & Mass Transfer, **5**, 897 (1962).

[24] Y.P. Shlykov and Y.A. Ganin, Int. J. Heat & Mass Transfer, **7**, 921 (1964).

[25] D.V. Lewis and H.C. Perkins, Int. J. of Heat & Mass Transfer, **11**, 1371 (1968).

[26] G.F. Hewitt et al., International Encyclopedia of Heat & Mass Transfer (CRC Press, New York, 1997).

[27] Mitsuhiro Matumoto et al, J. JSME (B), **68**, 87 (2002).

[28] S.H. Choi and S. Maruyama, Proc. of 39th National Heat Transfer Symp. of Japan (Sapporo, 2002).

[29] S.H. Choi and S. Maruyama, Proc. of 40th National Heat Transfer Symp. of Japan (Hiroshima, 2003).

[30] S.H. Choi, Ph. D. Thesis (The Univ. of Tokyo, 2003).

[31] Hideo Kaburaki et al., Proc. of Material Research Society Symp., **538**, 503 (1999).

[32] J.Q. Broughton and G.H. Gilmer, J. Chem. Phys., **70**, 5095 (1983).

[33] H. J. Pain, The Physics of Vibration and Waves (John Wiley & Sons, New York, 1983).